Multi-Pulse Pulse-Position-Modulation Signaling for Optical Communication with Direct Detection

M. K. Simon[1] and V. A. Vilnrotter[1]

A modification of the traditional pulse-position modulation (PPM) scheme typically employed on the optical direct-detection channel is proposed that allows for significantly improved information throughput and bandwidth advantage. The scheme sends a multitude (K) of pulses per symbol interval and as such provides a signal constellation whose size, for a given number of pulse slots (M), varies as M^K (for large M) rather than linearly with M, as is the case for conventional PPM. Maximum performance improvement is obtained for deep-space optical communications applications, where narrow high-peak-power transmitted pulses offer significant advantages in terms of detection probabilities and background suppression capabilities at the receiver.

I. Introduction

Pulse-position modulation, or PPM, is an accepted technique for transmitting information over the optical direct-detection channel [1,2]. At the transmitter, the encoder maps blocks of L consecutive binary symbols, or bits, into a single PPM channel symbol by placing a single laser pulse into one of $M = 2^L$ time slots. The PPM symbols are orthogonal, since there is no overlap between pulses in any pair of symbols. After establishing slot and symbol synchronization, the receiver detects the uncoded PPM symbols by determining which of the M slots contains the laser pulse, and performs the inverse mapping operation to recover the bit stream. Each correctly decoded PPM symbol conveys L bits of information; however, the receiver must operate with much greater bandwidth than the actual data rate to effect the decoding operation. If each bit is T_b seconds in duration, then L bits take LT_b seconds to transmit; this means the receiver must process 2^L PPM time slots in LT_b seconds to avoid overflow. The processing rate of the system (both transmitter and receiver) therefore must be a factor of $2^L/L$ times as great as the transmitted bit rate, implying a required bandwidth expansion by a corresponding amount. For large L, this bandwidth expansion can be severe, ultimately limiting the information throughput of the system due to limitations on the sampling rate.

A natural extension of single-pulse PPM is the use of two or more pulses to convey information in each channel symbol [3]. This can be accomplished by placing more than one pulse in all possible ways among

[1] Communications Systems Research Section.

The research described in this publication was carried out by the Jet Propulsion Laboratory, California Institute of Technology, under a contract with the National Aeronautics and Space Administration.

M slots, generating a much larger number of usable channel symbols when M is large; however, not all of the channel symbols are orthogonal, and the number of symbols in the set so generated is not necessarily a power of two, thus complicating the encoding operation. Nevertheless, multi-pulse PPM[2] has desirable properties, namely the potential for significantly reducing bandwidth requirements at fixed average power as compared to the "best" single-pulse PPM strategy, or increasing information throughput at a given bandwidth without incurring significant performance penalties.

In the next section, we shall examine the information throughput and bandwidth requirement properties of multi-pulse PPM, and compare it to both conventional single-pulse PPM and the "best" single-pulse PPM strategy that maximizes throughput with an average-power constraint. The maximum-likelihood strategy for optimally decoding multi-pulse PPM will be derived in Section III for direct-detected optical signals in the presence of multimode background radiation. Exact performance of two-pulse PPM will be determined in Section IV, both for the erasure channel (no background radiation) and for the general case with arbitrary background, and performance comparisons and numerical results will be presented in Section V.

II. Information Throughput and Bandwidth Requirements

With a single pulse placed in one of M slots, as with conventional PPM, the number of bits per PPM symbol is $\log_2 M$. The number of orthogonal symbols with "single-pulse PPM" is $\binom{M}{1} = M$. For the simple case of $M = 4$, the PPM symbols could be listed as

$$\begin{array}{cccc} 1 & 0 & 0 & 0 \\ 0 & 1 & 0 & 0 \\ 0 & 0 & 1 & 0 \\ 0 & 0 & 0 & 1 \end{array}$$

where each "1" represents a laser pulse, with an average of $K_s = \lambda_s \tau$ photons per pulse at the receiver. Here, τ denotes the duration of the PPM time slot and λ_s denotes the signal intensity in photons/second (assumed to be constant over the time slot).[3] Also, the symbol time associated with a single PPM transmission is $T_s = M\tau$, and thus the average signal power of such a transmission is K_s/T_s.

Suppose that instead of using a single PPM pulse we employ two pulses, and consider the number of possible "dual-pulse PPM" symbols that can be generated in this manner. The number of such symbols is clearly $\binom{M}{2} = [M(M-1)]/2$; however, not all dual-pulse PPM symbols are orthogonal, as the following example illustrates. For the case $M = 4$, the number of possible two-pulse symbols is 6:

$$\begin{array}{cccc} 1 & 0 & 0 & 1 \\ 0 & 1 & 1 & 0 \\ 0 & 1 & 0 & 1 \\ 1 & 0 & 1 & 0 \\ 1 & 1 & 0 & 0 \\ 0 & 0 & 1 & 1 \end{array}$$

[2] For the specific case of two pulses per channel symbol, we shall refer to this modulation scheme as either two-pulse PPM or dual-pulse PPM.

[3] The bandwidth of a particular modulation scheme is directly proportional to the inverse of the time slot duration. Thus, two modulation schemes having the same τ will occupy the same bandwidth. This fact will play an important role later on in the article when we deal with comparisons of the different modulation schemes.

Starting at the top, we proceed down and note that with the above arrangement the first two symbols are orthogonal; however, all the rest have one pulse overlap with the top two, and similarly for other pairs of orthogonal symbols. In general, we note that each two-pulse PPM symbol is orthogonal to $\binom{M-2}{2}$ other symbols, as can be seen by crossing out the columns occupied by the two laser pulses of any particular symbol: that leaves $(M-2)$ columns among which we can arrange two pulses in $\binom{M-2}{2}$ distinct ways, none of which has any overlap with the original symbol. The number of symbols not orthogonal with a given two-pulse PPM symbol is therefore $\binom{M}{2} - \binom{M-2}{2} - 1$. These relationships are easily verified for the above example with $M = 4$: the number of symbols orthogonal to any given two-pulse PPM symbol is 1, whereas the number of symbols not orthogonal to it is 4. We observe, however, that for large M any given two-pulse PPM symbol will be orthogonal to most of the remaining symbols; for example, with $M = 256$, any given symbol will be orthogonal to 32,131 other symbols, and not orthogonal to only 508 other symbols.

For conventional single-pulse PPM, the number of orthogonal symbols is equal to the number of slots, M; thus, the information throughput is $\log_2 M$ bits/symbol. As stated above, the number of symbols for two-pulse PPM is

$$\binom{M}{2} = \frac{M(M-1)}{2} \underset{M \gg 1}{\cong} \frac{M^2}{2}$$

With M slots, the two-pulse PPM set contains

$$N(2) = \log_2 M + \log_2(M-1) - \log_2 2 \underset{M \gg 2}{\cong} 2 \log_2 M \tag{1}$$

bits of information per symbol. The extension to "K-pulse PPM" is straightforward. The number of symbols generated by K pulses arranged in all possible patterns among M slots is

$$\binom{M}{K} = \frac{M!}{K!\,(M-K)!} \underset{M \gg K}{\cong} \frac{M^K}{K!} \tag{2}$$

Hence, the average number of bits per symbol is

$$N(K) = \sum_{i=0}^{K-1} \log_2(M-i) \; - \sum_{i=0}^{K} \log_2(K-i) \underset{M \gg K}{\cong} K \log_2 M \tag{3}$$

Thus, for the case $M >> K$, the information throughput has been increased by nearly a factor of K over single-pulse PPM with the same number of slots M. However, if each pulse contains the same average photon count as a single PPM pulse, then the average signal power, i.e., $K \times (K_s/T_s)$, has effectively been increased by a factor of K in order to achieve this gain. Perhaps, then, it might be more appropriate to compare each multi-pulse PPM symbol not just to a single PPM symbol with the same average photon count as one of the multi-pulse PPM symbols, but rather to a constellation of symbols composed of K consecutive single-pulse PPM symbols, each of symbol duration T_s/K and dimensionality M/K. This modulation scheme, which then has the same average energy per unit time, or equivalently the same average power as the previously described K-pulse PPM, shall be referred to as *compound-K single-pulse*

M-PPM.[4] By dividing the M slots into K groups, each occupying M/K slots and assigning a conventional single-pulse M/K PPM constellation to each group as was done in [3], then the number of compound-K single-pulse PPM symbols is $(M/K)^K$ with a corresponding throughput

$$N(K) = K \log_2 M - K \log_2 K \tag{4}$$

bits per symbol. Since $\binom{M}{K} \geq (M/K)^K, M > K$, it is clear that K-pulse PPM contains more symbols and hence conveys more information than compound-K single-pulse PPM since the latter is constrained to have no more than one pulse in any of the M/K slot symbols. The actual number of symbols and the corresponding information throughput for several values of K with $M = 256$ is shown in Table 1. It is clear that K-pulse PPM always improves upon single-pulse (conventional or compound) PPM in terms of information throughput, the improvement becoming significant as the number of pulses per symbol is increased.

Another way to compare these schemes is in terms of bandwidth required for the same information throughput. Denoting the total number of slots for K-pulse, compound-K single-pulse, and conventional single-pulse PPM by $M^{(A)}$, $M^{(B)}$, and $M^{(C)}$, respectively, then, analogous to the development in [3], equating the total number of symbols for the three schemes, their information throughputs are equal when

$$M^{(C)} = \left(\frac{M^{(B)}}{K}\right)^K = \binom{M^{(A)}}{K} \underset{M \gg K}{\cong} \frac{\left(M^{(A)}\right)^K}{K!} \tag{5}$$

Solving for $M^{(B)}$ in terms of $M^{(A)}$, for example, yields

$$M^{(B)} \cong \frac{K}{\sqrt[K]{K!}} M^{(A)} \tag{6}$$

Table 1. Comparison of the number of symbols and information throughput of three different PPM schemes: conventional single-pulse PPM, compound-*K* single-pulse PPM, and *K*-pulse PPM signal-sets; *M* = 256.

K	Compound-K single-pulse M-PPM, no. of symbols	K-pulse M-PPM, no. of symbols	Information throughput, conventional single-pulse M-PPM, bits/symbol	Information throughput, compound-K single-pulse M-PPM, bits/symbol	Information throughput, K-pulse M-PPM, bits/symbol
1	256	256	8	8	8
2	16,384	32,640	—	14	15
4	16,777,216	174,792,640	—	24	27.4
8	1.1×10^{12}	4.1×10^{14}	—	40	48.54

[4] We point out that an equivalent comparison to compound-K M-PPM is a comparison to conventional single-pulse M/K-PPM having symbol rate K/T_s. Specifically, both schemes have the identical bit rates, i.e., $(1/T_s)\log_2 (M/K)^K$ for the former and $(K/T_s)\log_2 (M/K)$ for the latter, and furthermore since the K symbols in compound-K PPM are independently chosen, optimal detection should yield identical bit-error rates (more about this later on in our discussion of performance).

The factor involving K on the right-hand side of Eq. (6) is equal to $\sqrt{2}$ when $K = 2$, and it approaches the number e as K approaches infinity. Since for a fixed symbol time, T_s, the slot time is given by $\tau = T_s/M$, then the above indicates that, in order to convey the same amount of information, compound-K single-pulse PPM requires significantly greater bandwidth than does K-pulse PPM. With limitations on digital sampling rates imposed by hardware considerations, this property of K-pulse PPM could become a significant factor for implementing high-data-rate telemetry.

III. Maximum-Likelihood Decision Metric

The maximum-likelihood metric for deciding optimally between an arbitrary number of intensity-modulated optical symbols, modulated according to any format whatsoever, has been previously derived [1]. Here we summarize the specific results pertinent to the problem under investigation in this article. It is assumed that Poisson statistics apply to both the detected signal and the detected background fields and to their sum when appropriate; this simplifying assumption is valid whenever a large number of space–time modes are observed and is generally true for signal-plus-background radiation under nominal operating conditions. The decision is based on a vector of time-disjoint count observables covering the symbol duration; here we assume that M distinct and disjoint counting intervals are sufficient to characterize each received symbol, and we base the decision on the M-component count vector $\mathbf{k} = (k_1, k_2, \cdots, k_M)$. We denote the ith hypothesis, corresponding to the ith distinct intensity-modulated symbol, by H_i. The probability of each count component is Poisson distributed with average value $K_b = \lambda_b \tau$ (λ_b denotes the background intensity) when only background radiation is observed, and $\lambda_{ij}\tau + K_b$ when both signal and background are present; here the subscript i refers to the hypothesis, whereas the subscript j identifies the observation interval within the count vector.

Since, conditioned on the intensity (hence the hypothesis), Poisson counts from disjoint intervals are independent, the joint probability for the count vector, conditioned on a given hypothesis, can be expressed as the product of the individual probabilities corresponding to each count:

$$P(\mathbf{k}|H_i) = \prod_{j=1}^{M} \frac{(\lambda_{ij}\tau + K_b)^{k_j}}{k_j!}\, e^{-(\lambda_{ij}+K_b)} \tag{7}$$

The maximum-likelihood decision rule is to compute the conditional probability for each hypothesis given the observed count vector and to select that hypothesis that yields the greatest value (i.e., that is most likely). The conditional probability, evaluated at the values of the observed count vector, is called the likelihood function. Since the logarithm is a monotone-increasing function of its argument, a much simpler computation may result if we equivalently base the decision on the "log-likelihood function," which is the natural logarithm of Eq. (7). Denoting the ith log-likelihood function by Λ_i, the decision can be based on the metrics obtained by evaluating Λ_i for each hypothesis and selecting the one that achieves the greatest value. Thus, we compute

$$\Lambda_i \equiv \ln P(\mathbf{k}|H_i) = \sum_{j=1}^{M} k_j \ln(\lambda_{ij}\tau + K_b) - \sum_{j=1}^{M} \ln(k_j!) - \sum_{j=1}^{M} (\lambda_{ij}\tau + K_b) \tag{8}$$

Note that the second term on the right-hand side of Eq. (8) does not depend on the hypothesis, and hence cannot contribute to the decision; this term can be ignored. The third term on the right-hand side of Eq. (8) is the total energy of the signal and background for the ith symbol, which we denote by E_i. This term contributes to the decision only if the total symbol energy depends on the hypothesis; otherwise, for the case of equal-energy symbols, it too can be ignored. Observe that the first term on the right-hand side of Eq. (8) can be rewritten in a slightly different form, by dividing by the background energy:

$$\sum_{j=1}^{M} k_j \ln(\lambda_{ij}\tau + K_b) = \sum_{j=1}^{M} k_j \ln\left(1 + \frac{\lambda_{ij}\tau}{K_b}\right) + \sum_{j=1}^{M} k_j \ln(K_b) \tag{9}$$

Again, the second term on the right-hand side of Eq. (9) is independent of the hypothesis; hence, it can be ignored. Taking these simplifications into account, the log-likelihood function for the general case can be rewritten as

$$\Lambda_i = \sum_{j=1}^{M} k_j \ln\left(1 + \frac{\lambda_{ij}\tau}{K_b}\right) - E_i \tag{10}$$

where E_i is the energy associated with the ith hypothesis. Next, we apply these results to the case of two-pulse PPM and determine its performance, first with negligible background and then in the presence of background radiation.

IV. Performance

The decision rule derived above is defined in terms of log-likelihood metrics consisting of the sum of logarithmically weighted counts obtained from each "signal slot" of the various hypotheses. The decision rule is to select that hypothesis corresponding to the greatest log-likelihood function, given the vector of observables. For the special case of equal-energy signal pulses, the logarithmic weights for all likelihood functions are exactly the same, and hence can be ignored. This means that the log-likelihood functions consist of the sum of counts from all possible patterns of two slots among the M slots available for each symbol.

The symbol-error probability performance of conventional single-pulse PPM is well known and is repeated here for reference in the form derived in [4], namely,

$$P_s(E) = 1 - \frac{1}{M} e^{-(K_s + MK_b)} - \sum_{k=1}^{\infty} \frac{(K_s + K_b)^k}{k!} \left[\sum_{l=0}^{M-1} \frac{1}{l+1} \binom{M-1}{l} \left(\frac{K_b^k}{k!}\right)^l \left(\sum_{j=0}^{k-1} \frac{K_b^j}{j!} \right)^{M-1-l} \right]$$

$$\times\, e^{-(K_s + MK_b)} \tag{11}$$

where $K_s = \lambda_s \tau$ and λ_s is the signal intensity. An alternative form for Eq. (11) can be obtained by making use of the combinatorial identity

$$\sum_{l=0}^{M-1} \frac{1}{l+1} \binom{M-1}{l} a^l b^{M-2-l} = \frac{(a+b)^M - b^M}{aM} \tag{12}$$

resulting in[5]

$$P_s(E) = 1 - \frac{1}{M} \sum_{k=0}^{\infty} \left(\frac{K_s + K_b}{K_b} \right)^k \left[\left(\sum_{j=0}^{k} \frac{K_b^j}{j!} \right)^M - \left(\sum_{j=0}^{k-1} \frac{K_b^j}{j!} \right)^M \right] e^{-(K_s + MK_b)} \tag{13}$$

[5] J. Hamkins, "Accurate Computation of the Performance of M-ary Orthogonal Signaling on a Discrete Memoryless Channel," Jet Propulsion Laboratory, Pasadena, California, submitted to *IEEE Trans. Letters*.

Although Eq. (13) is more compact than Eq. (11), numerical results obtained from the former tend to be inaccurate at large values of K_s (relative to K_b) due to the fact that, for large values of the summation index k, the term in brackets corresponds to the difference of two numbers that are very close to one another. A way around this difficulty has been suggested.[6] However, for our numerical evaluation purposes here, we will continue to use the form in Eq. (11) .

Another possible simplification is the replacement of the third sum in Eq. (11) [equivalently, the second and third sums in Eq. (13)] by known tabulated functions, i.e.,

$$\sum_{j=0}^{k_1-1} \frac{K_b^j}{j!} = e^{K_b} Q_{k_1}\left(0, \sqrt{2K_b}\right) = e^{K_b} \frac{\Gamma\left(k_1, K_b\right)}{\Gamma\left(k_1\right)} \tag{14}$$

where $Q_m\left(\alpha, \beta\right)$ is the mth order Marcum Q-function [5] and $\Gamma\left(n, k\right)$ is the incomplete gamma function [6]. Once again, for numerical evaluation purposes, this simplification does not appear to offer any strong advantage.

We now proceed to derive an expression for the equivalent-performance characterization of dual-pulse PPM. Our goal is to obtain an exact expression for the average symbol-error probability performance of this modulation scheme in contrast to an upper bound on such performance obtained previously [7]. Aside from the obvious analytical satisfaction, an exact expression will allow more accurate numerical results to be obtained for small values of M. With no loss in generality, we shall assume that the first hypothesis is true, denoted by H_1, corresponding to the transmission of laser pulses in the first and second of the M slots.

A. Negligible Background Radiation

We begin by first considering the performance of dual-pulse PPM for the noiseless case, so as to introduce the key underlying concepts that will have to be generalized when we relax this constraint. The number of two-pulse patterns among M slots is equal to $\binom{M}{2} = [M(M-1)]/2$. Because of symmetry, we assign equal a priori probabilities to all hypotheses, so that the probability of the ith two-pulse pattern occurring is $P(H_i) = \binom{M}{2}^{-1} = 2/[M(M-1)]$.

The following are the events that arise in the analysis of the error-probability performance of dual-pulse PPM. Under the condition of negligible background radiation, photon counts only can occur in the signal slots, but detection of no photon counts in either or both of the signal slots is also possible due to the non-zero probability of getting zero counts with the assumed Poisson statistics. The probability of getting zero counts in the slots that do not contain the signal is one, since we assumed zero average background energy. Therefore, the probability of getting (a) a count of one or more in the first two slots (taken to be the signal slots for hypothesis H_1) and zero everywhere else is

$$P(k_1 \geq 1, k_2 \geq 1, k_3 \text{ through } k_M = 0) = \left(1 - e^{-K_s}\right)^2 \tag{15}$$

When this event occurs, the transmitted hypothesis is identified correctly with probability one. However, it is also possible to (b) receive a non-zero count in the first slot but no counts in the second slot, (c) receive a non-zero count in the second slot but no count in the first slot, or (d) receive no counts in either signal slot, hence no counts over the entire observation vector. The probabilities of these events are

[6] Ibid.

$$P(k_1 \geq 1, k_2 = 0, k_3 \text{ through } k_M = 0) = P(k_1 = 0, k_2 \geq 1, k_3 \text{ through } k_M = 0)$$

$$= e^{-K_s}\left(1 - e^{-K_s}\right) \tag{16}$$

$$P(k_1 = 0, k_2 = 0, k_3 \text{ through } k_M = 0) = e^{-2K_s} \tag{17}$$

When (b) or (c) occurs, there is no clear decision strategy, because we do not have enough information to distinguish between those patterns that have a signal pulse in the first (or second) slot; in this case, optimality is not compromised by choosing randomly among the remaining possibilities. Since the number of patterns with a pulse in the first (or second) slot is $(M-1)$, a random choice among these possibilities yields a correct decision with probability $1/(M-1)$. Similarly, when event (d) occurs, a random choice among all possibilities yields a correct decision with probability $[M(M-1)/2]^{-1}$. Considering all possibilities, the probability of a correct decision in the absence of background radiation is

$$P(C|H_1) = \left(1 - e^{-K_s}\right)^2 + \frac{2}{M-1}e^{-K_s}\left(1 - e^{-K_s}\right) + \frac{2}{M(M-1)}e^{-2K_s}$$

$$= 1 - 2\left(\frac{M-2}{M-1}\right)e^{-K_s} + \left(\frac{M-2}{M}\right)e^{-2K_s} \tag{18}$$

Note that for $M = 2$ we get $P(C|H_1) = 1$, meaning that we always choose correctly; however, since with dual-pulse PPM there can be only one hypothesis in this case, there is no transfer of information. Finally, since the result in Eq. (18) is independent of the hypothesis chosen, the average symbol-error probability is given by

$$P_s(E)\,|_{\text{dual pulse}} = 2\frac{M-2}{M-1}e^{-K_s} - \frac{M-2}{M}e^{-2K_s} \tag{19}$$

For conventional single-pulse PPM, the corresponding relationship to Eq. (19) is

$$P_s(E)\,|_{\text{conv. PPM}} = \frac{M-1}{M}e^{-K_s} \tag{20}$$

Thus, for a given value of K_s, we observe that in the limit of large M and large K_s, single-pulse PPM will outperform dual-pulse PPM by as much as a factor of two in symbol-error probability.

For compound-2 single-pulse PPM, a correct symbol decision requires that both pulses from the two consecutive single-pulse $M/2$ PPM constellations be correctly detected. Thus, the probability of error for this modulation scheme is

$$P_s(E)\,|_{\text{comp. PPM}} = 1 - \left(1 - P_s(E)\left|_{\substack{\text{conv. PPM} \\ M \to M/2}}\right.\right)^2 = 2P_s(E)\left|_{\substack{\text{conv. PPM} \\ M \to M/2}}\right. - \left(P_s(E)\left|_{\substack{\text{conv. PPM} \\ M \to M/2}}\right.\right)^2 \tag{21}$$

In other words, the probability of an error in the compound symbol is equal to the probability of error in the first pulse (with the second pulse correct or not), plus the probability the second pulse is in error (with the first pulse correct or not), and since this sum contains the simultaneous (squared) error term twice, we need to subtract out one of the squared error terms in order to obtain the exact error probability. Here again, for a given value of K_s, we observe that, in the limit of large M, compound-2 single-pulse PPM will approach the performance of dual-pulse PPM.

B. Non-Negligible Background Radiation

To begin the discussion, we point out that if any of the noise-only slots contain a number of counts greater than the smaller of the number of counts in the two signal slots, then the signal slot containing this smaller number of counts will not be included as part of the slot-pair decision, i.e., a decision error will occur. Mathematically speaking, if for any $i = 3, 4, \cdots, M$, $k_i > \min(k_1, k_2)$, then such an event cannot contribute to the probability of correct detection. With this in mind, we now spell out the various events that contribute to this probability when background radiation is included.

Event 1. One or more photons are detected in slots 1 and 2 ($k_1, k_2 \geq 1$) and all other $M-2$ slots have fewer detected photons than in either slot 1 or 2 $\big(k_3, k_4, \cdots, k_M < \min(k_1, k_2)\big)$. Here a correct decision will be made with certainty and, thus, the contribution of this event to the probability of a correct decision corresponds to the probability of occurrence of the event itself, namely,

$$P_1(C) = \sum_{k_1=1}^{\infty} \frac{(K_s + K_b)^{k_1}}{k_1!} e^{-(K_s+K_b)} \sum_{k_2=1}^{\infty} \frac{(K_s + K_b)^{k_2}}{k_2!} e^{-(K_s+K_b)} \left(\sum_{j=0}^{k_{\min}-1} \frac{K_b^j}{j!} e^{-K_b} \right)^{M-2} \tag{22}$$

where $k_{\min} = \min(k_1, k_2)$.

Event 2. An unequal number (but at least one) of photons are detected in slots 1 and 2 ($k_1 \neq k_2 \geq 1$); any other $l = 1, 2, 3, \cdots, M-2$ slots have $k_{\min} = \min(k_1, k_2)$ detected photons; and the remaining $M-l-2$ slots have less than $k_{\min}$ detected photons. This event can occur in $\binom{M-2}{l}$ ways (corresponding to the number of possible combinations of the l noise-only slots that contain $k_{\min}$ detected photons). Furthermore, a correct decision is no longer guaranteed since there now are $l+1$ equally likely ways for a slot (other than the signal slot not corresponding to $k_{\min}$) to have $k_{\min} > 0$ detected photons, only one of which produces the true correct decision. Thus, the contribution to the probability of correct decision stemming from this event is

$$P_2(C) = \sum_{l=1}^{M-2} \frac{1}{l+1} \binom{M-2}{l} \sum_{k_1=1}^{\infty} \frac{(K_s + K_b)^{k_1}}{k_1!} e^{-(K_s+K_b)} \sum_{\substack{k_2=1 \\ k_2 \neq k_1}}^{\infty} \frac{(K_s + K_b)^{k_2}}{k_2!} e^{-(K_s+K_b)}$$

$$\times \left(\frac{K_b^{k_{\min}}}{k_{\min}!} e^{-K_b} \right)^l \left(\sum_{j=0}^{k_{\min}-1} \frac{K_b^j}{j!} e^{-K_b} \right)^{M-2-l} \tag{23}$$

Event 3. An equal number (but at least one) of photons are detected in slots 1 and 2 ($k_1 = k_2 = k \geq 1$); any other $l = 1, 2, 3, \cdots, M-2$ slots have k detected photons; and the remaining $M-l-2$ slots have less than k detected photons. (Note that k also could be denoted by $k_{\min} = \min(k_1, k_2)$ since k_1 and k_2 are equal. This will be convenient later on when combining events.) This event can occur in $\binom{M-2}{l}$ ways (corresponding to the number of possible combinations of the l noise-only slots that contain k detected photons). Furthermore, a correct decision is no longer guaranteed since there now are $\binom{l+2}{2}$ equally likely ways for a pair of slots to have $k > 0$ detected photons, only one of which produces the true correct decision. Thus, the contribution to the probability of correct decision stemming from this event is

$$P_3(C) = \sum_{l=1}^{M-2} \binom{l+2}{2}^{-1} \binom{M-2}{l} \sum_{k=1}^{\infty} \left(\frac{(K_s+K_b)^k}{k!} e^{-(K_s+K_b)} \right)^2 \left(\frac{K_b^k}{k!} e^{-K_b} \right)^l$$

$$\times \left(\sum_{j=0}^{k-1} \frac{K_b^j}{j!} e^{-K_b} \right)^{M-2-l} \tag{24}$$

Event 4. One or more photons are detected in slot 1 ($k_1 \geq 1$), and all other slots have zero detected photons. Furthermore, a correct decision is no longer guaranteed since there now are $\binom{M-1}{1} = M-1$ equally likely ways for a slot (other than the first) to have zero detected photons, only one of which produces the true correct decision. Thus, the contribution to the probability of correct decision stemming from this event is

$$P_4(C) = \frac{1}{M-1} \left[\sum_{k_1=1}^{\infty} \frac{(K_s+K_b)^{k_1}}{k_1!} e^{-(K_s+K_b)} \right] e^{-(M-2)K_b} e^{-(K_s+K_b)}$$

$$= \frac{1}{M-1} \left(e^{K_s+K_b} - 1 \right) e^{-(2K_s+MK_b)} = \frac{1}{M-1} \left(e^{-(K_s+(M-1)K_b)} - e^{-(2K_s+MK_b)} \right) \tag{25}$$

Event 5. This is the counterpart to Event 4—one or more photons are detected in slot 2 ($k_2 \geq 1$), and all other slots have zero detected photons. By symmetry, the probability of correct decision, $P_5(C)$, stemming from this event is identical to $P_4(C)$.

Event 6. All slots have zero detected counts. Here a random decision among $\binom{M}{2} = [M(M-1)]/2$ possible slot pairs is made, resulting in a contribution to the probability of correct decision of

$$P_6(C) = \frac{2}{M(M-1)} \left[e^{-(K_s+K_b)} \right]^2 e^{-(M-2)K_b} = \frac{2}{M(M-1)} e^{-(2K_s+MK_b)} \tag{26}$$

Examination of the probability of Event 1 as given in Eq. (22) reveals that it can be included in Event 2 and Event 3 by allowing the summation on l in Eqs. (23) and (24) to run from zero to infinity instead of one to infinity. Then the total probability of correct detection is obtained from the sum of Eq. (23) and Eq. (24) (modified as above) through Eq. (26). Some simplification of the various terms that contribute to this summation is possible; however, before proceeding with this and discussing its value in regard to numerical evaluation, we first check that the end result agrees with the result previously obtained for the special case of no background noise, i.e., $K_b = 0$. For this special case, each of the contributing probabilities is evaluated as follows.

For Event 1, only the $j = 0$ term in the third sum survives. Thus, from Eq. (22),

$$P_1(C) = \left(\sum_{k_1=1}^{\infty} \frac{K_s^{k_1}}{k_1!} e^{-K_s} \right) \left(\sum_{k_2=1}^{\infty} \frac{K_s^{k_2}}{k_2!} e^{-K_s} \right) = \left(e^{K_s} - 1 \right)^2 e^{-2K_s} \tag{27}$$

The probabilities corresponding to Events 2 and 3 are equal to zero. For the equiprobable Events 4 and 5, we have

$$P_4(C) + P_5(C) = \frac{2}{M-1}\left(e^{-K_s} - e^{-2K_s}\right) \tag{28}$$

Finally, for Event 6 we obtain

$$P_6(C) = \frac{2}{M(M-1)}e^{-2K_s} \tag{29}$$

Thus, summing up Eqs. (27) through (29) gives

$$P(C) = 1 - 2\left(\frac{M-2}{M-1}\right)e^{-K_s} + \frac{M-2}{M}e^{-2K_s} \tag{30}$$

which agrees with the previously obtained result in Eq. (18).

Including Eq. (22) as the $l = 0$ term in Eqs. (23) and (24) as discussed above and reordering the summations, we obtain

$$P_1(C) + P_2(C) + P_3(C) = \sum_{k_1=1}^{\infty}\frac{(K_s+K_b)^{k_1}}{k_1!}\sum_{k_2=1}^{\infty}\frac{(K_s+K_b)^{k_2}}{k_2!}$$
$$\times\left[\sum_{l=0}^{M-2} I(l,k_1,k_2)\binom{M-2}{l}\left(\frac{K_b^{k_{\min}}}{k_{\min}!}\right)^l\left(\sum_{j=0}^{k_{\min}-1}\frac{K_b^j}{j!}\right)^{M-2-l}\right]e^{-(2K_s+MK_b)} \tag{31}$$

where

$$I(l,k_1,k_2) = \begin{cases}\dfrac{1}{l+1}, & k_1 \neq k_2\\[2ex] \dbinom{l+2}{2}^{-1} = \dfrac{2}{(l+2)(l+1)}, & k_1 = k_2\end{cases} \tag{32}$$

Finally, summing Eqs. (25) through (27), adding the result to Eq. (31) and subtracting from 1, we obtain the desired expression for average symbol-error probability, namely,

$$P_s(E) = 1 - \frac{2}{M-1}e^{-(K_s+(M-1)K_b)} + \frac{2}{M}e^{-(2K_s+MK_b)} - \sum_{k_1=1}^{\infty}\frac{(K_s+K_b)^{k_1}}{k_1!}\sum_{k_2=1}^{\infty}\frac{(K_s+K_b)^{k_2}}{k_2!}$$
$$\times\left[\sum_{l=0}^{M-2} I(l,k_1,k_2)\binom{M-2}{l}\left(\frac{K_b^{k_{\min}}}{k_{\min}!}\right)^l\left(\sum_{j=0}^{k_{\min}-1}\frac{K_b^j}{j!}\right)^{M-2-l}\right]e^{-(2K_s+MK_b)} \tag{33}$$

With some abuse of the notation, it is possible to write Eq. (33) in yet a more compact form that incorporates the second and third terms in the summations on k_1 and k_2. In particular, after some manipulation it can be shown that

$$P_s(E) = 1 - \sum_{k_1=0}^{\infty} \frac{(K_s+K_b)^{k_1}}{k_1!} \sum_{k_2=0}^{\infty} \frac{(K_s+K_b)^{k_2}}{k_2!}$$

$$\times \left[\sum_{l=0}^{M-2} I(l,k_1,k_2) \binom{M-2}{l} \left(\frac{K_b^{k_{\min}}}{k_{\min}!} \right)^l \left(\sum_{j=0}^{k_{\min}-1} \frac{K_b^j}{j!} \right)^{M-2-l} \right] e^{-(2K_s+MK_b)} \tag{34}$$

where it is understood that, if $k_{\min} = 0$, then the summation on j equals zero, and thus $\left(\sum_{j=0}^{k_{\min}-1} [K_b^j/j!]\right)^{M-2-l} = 0$ unless $l = M-2$, in which case $\left(\sum_{j=0}^{k_{\min}-1}[K_b^j/j!]\right)^{M-2-l} = 1$.

Due to the symmetry of Eq. (33) or Eq. (34) in k_1 and k_2, it is possible to reduce the infinite sum on one of these indices to a finite sum. In particular, the double sum $\sum_{k_1=1}^{\infty}\sum_{k_2=1}^{\infty}(\cdot)$ can be replaced by $2\sum_{k_1=2}^{\infty}\sum_{k_2=1}^{k_1-1}(\cdot) + \sum_{k_1=1}^{\infty}(\cdot)\big|_{k_2=k_1}$, leading to the simplification

$$P_s(E) = 1 - \frac{2}{M-1} e^{-(K_s+(M-1)K_b)} + \frac{2}{M} e^{-(2K_s+MK_b)} - 2\sum_{k_1=2}^{\infty} \frac{(K_s+K_b)^{k_1}}{k_1!} \sum_{k_2=1}^{k_1-1} \frac{(K_s+K_b)^{k_2}}{k_2!}$$

$$\times \left[\sum_{l=0}^{M-2} \frac{1}{l+1} \binom{M-2}{l} \left(\frac{K_b^{k_2}}{k_2!} \right)^l \left(\sum_{j=0}^{k_2-1} \frac{K_b^j}{j!} \right)^{M-2-l} \right] e^{-(2K_s+MK_b)}$$

$$- \sum_{k=1}^{\infty} \left[\frac{(K_s+K_b)^k}{k!} \right]^2 \left[\sum_{l=0}^{M-2} \frac{2}{(l+1)(l+2)} \binom{M-2}{l} \left(\frac{K_b^k}{k!} \right)^l \left(\sum_{j=0}^{k-1} \frac{K_b^j}{j!} \right)^{M-2-l} \right] e^{-(2K_s+MK_b)} \tag{35}$$

Once again it is possible to apply the relation in Eq. (12) to algebraically simplify the term on the second line of Eq. (35). However, as previously mentioned, this simplification potentially leads to computational inaccuracy and thus for the purpose of our numerical results we shall use the form given in Eq. (35).

The performance of dual-pulse PPM and its comparison with that of the conventional and compound single-pulse PPM approaches under average-power, peak-power, and bandwidth constraints is the subject of the next section.

V. Numerical Results

The advantages of multi-pulse PPM over the best single-pulse strategy in terms of information throughput have been described in Section II. However, throughput is not the only criterion for evaluating and comparing modulation formats; performance also must be taken into account. Since single-pulse PPM is a completely orthogonal modulation while dual- or multi-pulse PPM is only partially orthogonal, performance degradation for the multi-pulse modulation formats is expected since not all of the energy is

available for differentiating between non-orthogonal symbols. For example, in the case of two-pulse PPM, where the maximum overlap between non-orthogonal pulses is equal to the energy of one pulse, only half of the energy is used to differentiate between the correct pulse and competing non-orthogonal pulses. On the other hand, multi-pulse PPM signals contain more channel symbols than do the corresponding repeated single-pulse PPM sets, and therefore enjoy a bandwidth advantage when equal throughput is the design criteria. In view of the above discussion, performance should be compared both at equal bandwidth and at equal information throughput. Finally, since increased bandwidth (narrower slot time) necessitates greater peak signal power to maintain constant average pulse energy, average-power and peak-power constraints also should be applied when comparing single-pulse and multi-pulse PPM signals.

The performance of single-pulse (conventional or compound) PPM can be compared with multi-pulse PPM symbols in several ways, namely, under a bandwidth constraint or under an information throughput constraint; each of these can further be divided into average-power-constrained or peak-power-constrained signals. For the purpose of numerical comparison, we consider only the case of $K = 2$. To facilitate the notation associated with the various comparisons, and to be consistent with notation used earlier in this article, we shall assign the superscripts (A), (B), and (C) to the parameters associated with dual-pulse, compound-2 single pulse, and conventional PPM modulations, respectively.

A. Peak-Power Constraint

The first set of comparisons to be made assumes that we impose a *peak-power* constraint on the signal, i.e., $\lambda_s^{(A)} = \lambda_s^{(B)} = \lambda_s^{(C)} \triangleq \lambda_s$. The peak-power constraint is particularly important in deep-space optical communications applications, where narrow high-peak-power transmitted pulses offer significant advantages in terms of detection probabilities and background-suppression capabilities at the receiver. However, the generation of high peak powers is ultimately limited by breakdown in materials and coatings, especially where erbidium-doped fiber amplifiers are employed—the optical field in these fiber amplifiers often reaches intensities so great that catastrophic damage occurs. Therefore, operation with a peak-power constraint below the damage threshold is required, and, hence, modulation formats capable of delivering high information throughput under a peak-power constraint are highly desirable in deep-space applications.

1. The Case of Equal Bandwidths. Requiring that all three schemes have equal bandwidths is equivalent to requiring that they have identical slot durations, i.e., $\tau^{(A)} = \tau^{(B)} = \tau^{(C)}$, or, since the symbol time is fixed, the equivalent relation, $M^{(A)} = M^{(B)} = M^{(C)} = M$. Combining this with the peak-power constraint given above is tantamount to setting $K_s^{(A)} = K_s^{(B)} = K_s^{(C)} \triangleq K_s$. Also, since the background radiation intensity is fixed at λ_b, then we also have $K_b^{(A)} = K_b^{(B)} = K_b^{(C)} \triangleq K_b$. A pictorial representation of the modulations for this case is given in Fig. 1 for $M = 16$, which depicts conventional single-pulse PPM, compound-2 single-pulse PPM formed from two single-pulse PPM symbols each of dimension $M/2 = 8$, and a typical two-pulse PPM symbol all chosen from constellations using a total of 16 equal-duration slots. The symbol-error probability of the three schemes is plotted in Fig. 2 versus $K_s = \lambda_s \tau$ (peak power normalized by the slot time or, equivalently, the energy per pulse) for $M = 16$ and $K_b = 0$, 0.1, and 0.5. Solid curves refer to dual-pulse PPM, dotted–dashed curves to conventional single-pulse PPM, and dashed curves to the corresponding compound symbol formed from the pair of single-pulse PPM symbols of half the dimension. The expressions used to arrive at these plots are given by Eqs. (19) through (21) for $K_b = 0$ and Eqs. (11), (21), and (33) for $K_b \neq 0$. We observe that, consistent with the previous discussion in Section IV, dual-pulse and compound-2 pulse PPM both perform worse than conventional single-pulse PPM, dual-pulse being the more inferior (approximately a factor of two in symbol-error probability). Again the reader is reminded of the fact that, with an equal bandwidth constraint, even for M equal only to 16, the information throughput of dual-pulse PPM is still somewhat higher than that of conventional or even compound-2 PPM. In particular, the numbers of bits per symbol for the three cases are $\log_2 \binom{16}{2} = 6.907$, $\log_2 (16/2)^2 = 6$, and $\log_2 16 = 4$, which represents a valuable trade-off against the relatively small penalty in symbol probability performance.

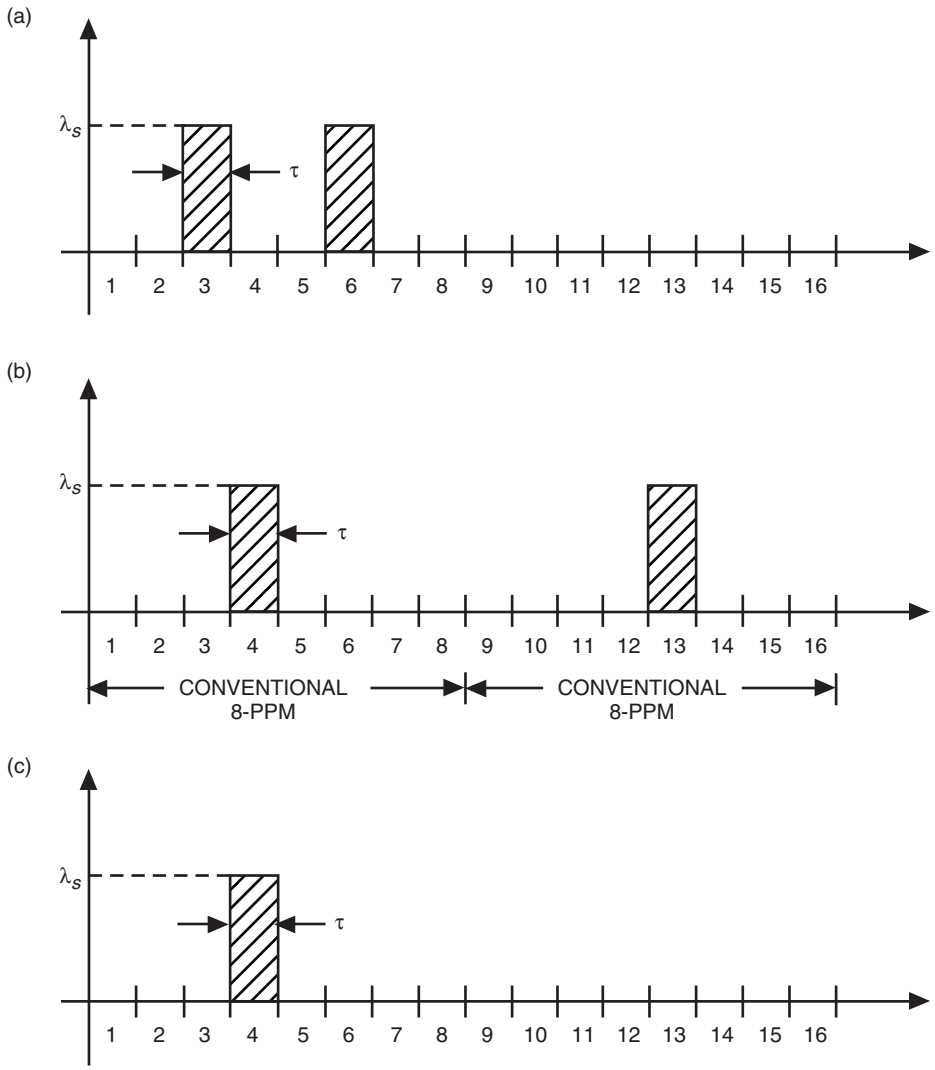

Fig. 1. An illustration of three different PPM modulation schemes with equal bandwidths and peak power levels, $M = 16$: (a) dual 16-PPM, (b) compound-2 16-PPM, and (c) conventional 16-PPM.

An alternative way of characterizing the performance for this case, which also takes into account the difference in information throughputs of the three schemes, is to consider a plot of bit-error probability versus peak power (normalized by the slot time) per bit, i.e., $\lambda_s \tau / N$ where, as before, N denotes the bits/symbol for each scheme as given in Section II. The conversion of the y-axis (ordinate) of Fig. 2 from symbol- to bit-error probability is, in principle, dependent on the modulation scheme. Since conventional single-pulse PPM is truly an orthogonal modulation scheme, then one can apply the well-known relation between symbol- and bit-error probability for such a scheme, namely, [8, Chapter 4, Eq. (4.96)]:

$$P_b(E) = \frac{1}{2}\left(\frac{M^{(C)}}{M^{(C)}-1}\right) P_s(E) \tag{36}$$

Although compound-2 single-pulse PPM and dual-pulse PPM are not truly orthogonal modulation schemes, for large M the number of symbols that are not orthogonal to a given member of the signal constellation becomes quite small relative to the number that are indeed orthogonal. Thus, to a

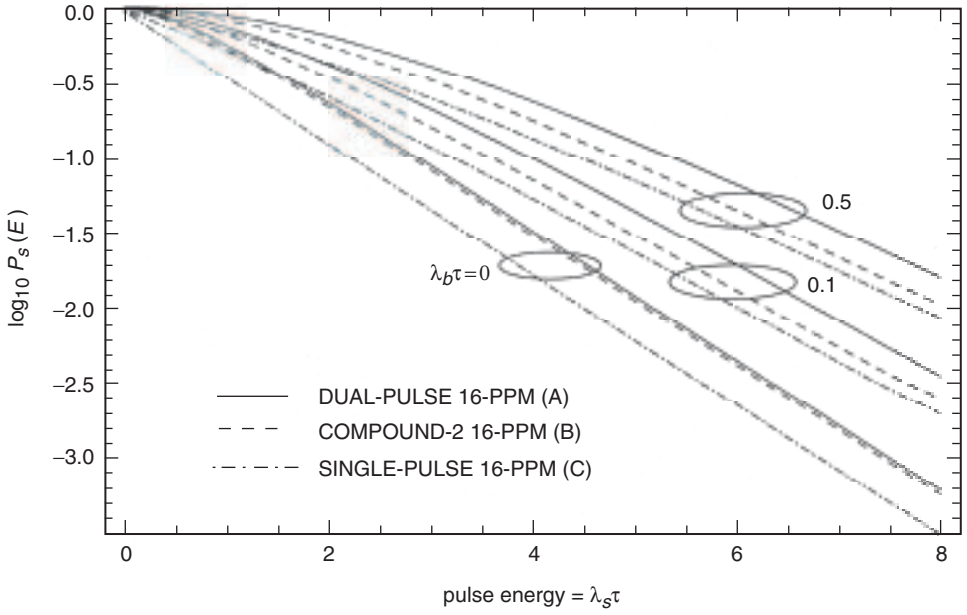

Fig. 2. Average symbol-error probability versus normalized peak power for conventional single, compound single, and dual-pulse PPM with normalized background power as a parameter; equal bandwidths.

first-order approximation, one can apply the same relation to these two modulation forms, accepting as well the fact that the number of bits per symbol may not always be integer. Thus, for compound-2 single-pulse PPM, we have

$$P_b(E) \cong \frac{1}{2}\left[\frac{(M^{(B)}/2)^2}{(M^{(B)}/2)^2 - 1}\right] P_s(E) \tag{37}$$

whereas for dual-pulse PPM we have

$$P_b(E) \cong \frac{1}{2}\left[\frac{M^{(A)}\left(M^{(A)}-1\right)/2}{M^{(A)}\left(M^{(A)}-1\right)/2 - 1}\right] P_s(E) \tag{38}$$

For the case at hand, $M^{(A)} = M^{(B)} = M^{(C)} = 16$, and thus these conversions become $P_b(E) = (8/15)P_s(E)$ for conventional single-pulse PPM, $P_b(E) \cong (32/63)P_s(E)$ for compound-2 single-pulse PPM, and $P_b(E) \cong (60/119)P_s(E)$ for dual-pulse PPM, all of which are close to $P_b(E) = (1/2)P_s(E)$. The resulting plot is provided in Fig. 3. Here we see that dual-pulse PPM is the best performer of the three, particularly when compared to conventional single-pulse M-PPM. Note that the bit-error probability of compound-2 M-PPM is identical to that of conventional single-pulse $(M/2)$-PPM as explained in Footnote 4, and thus the exact expression for this probability could be obtained from Eq. (11) with M replaced by $M/2$ combined with Eq. (36).

2. The Case of Equal Information Throughputs per Symbol. Suppose now that we compare the three schemes based on equal information throughputs as characterized by Eq. (11) but still maintain the same peak-power constraint. Then, if the symbol time is fixed, by necessity the bandwidths of the three schemes will be different. In particular, relative to the slot width of single-pulse conventional PPM, $\tau^{(C)}$, we have

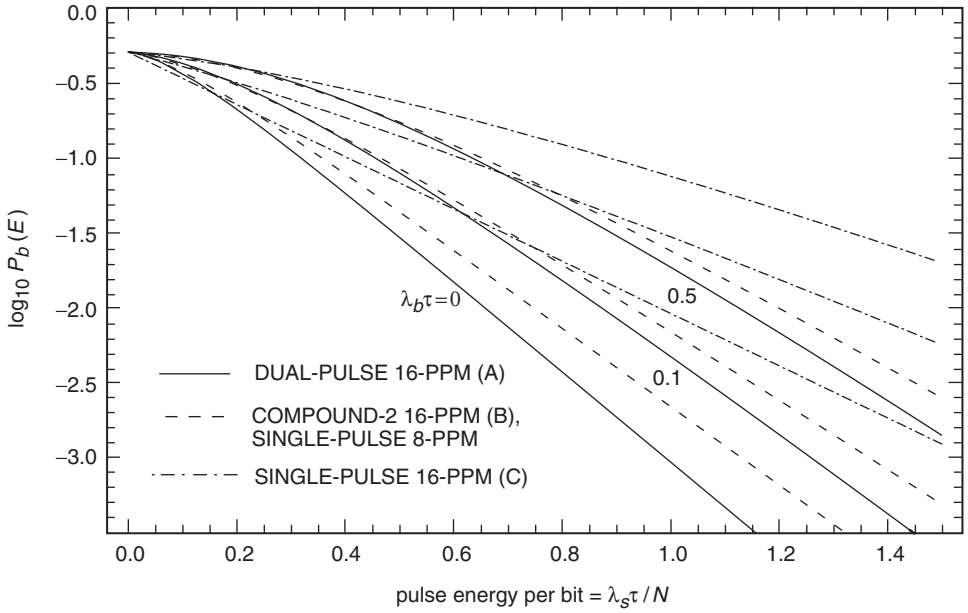

Fig. 3. Average bit-error probability versus normalized peak power per bit for conventional single, compound single, and dual-pulse PPM with normalized background power as a parameter; equal bandwidths.

$$\left.\begin{aligned} \tau^{(A)} &= \tau^{(C)}\left(\frac{M^{(C)}}{M^{(A)}}\right) = \tau^{(C)}\left(\frac{M^{(A)}-1}{2}\right) \\ \tau^{(B)} &= \tau^{(C)}\left(\frac{M^{(C)}}{M^{(B)}}\right) = \tau^{(C)}\left(\frac{M^{(B)}}{4}\right) \end{aligned}\right\} \tag{39}$$

or, equivalently, in terms of the normalized average signal energy of the single-pulse PPM scheme, $K_s^{(C)} = \lambda_s \tau^{(C)}$,

$$\left.\begin{aligned} K_s^{(A)} &= K_s^{(C)}\left(\frac{M^{(A)}-1}{2}\right) \\ K_s^{(B)} &= K_s^{(C)}\left(\frac{M^{(B)}}{4}\right) \end{aligned}\right\} \tag{40}$$

that is, the probability distributions characterizing the signal photon counts of the three different modulations schemes now have different Poisson parameters. Similarly, because of the unequal slot widths, we also have

$$\left.\begin{aligned} K_b^{(A)} &= K_b^{(C)}\left(\frac{M^{(A)}-1}{2}\right) \\ K_b^{(B)} &= K_b^{(C)}\left(\frac{M^{(B)}}{4}\right) \end{aligned}\right\} \tag{41}$$

A comparison of the symbol-error probability performances of the three different cases under a peak-power constraint and equal information throughputs is illustrated in Fig. 4 for dual-pulse PPM with $M^{(A)} = 16$, which, from the relation in Eq. (11), results in $M^{(B)} \cong 22$ for compound-2 single-pulse PPM and $M^{(C)} = 120$ for conventional single-pulse PPM. The curves in the plot depict average symbol-error probability versus $K_s^{(C)} = \lambda_s \tau^{(C)}$ (the energy per pulse of conventional single-pulse PPM) with $K_b^{(C)} = \lambda_b \tau^{(C)}$ as a parameter. From the results in this figure, we see the dramatic improvement in error-probability performance achieved by dual-pulse PPM as compared with the other two schemes over and above the bandwidth advantage described by Eq. (39).

B. Average-Power Constraint

For the second set of comparisons, we impose an *average-power* constraint on the signal. Unlike the peak-power constraint examined above, an average-power constraint usually is not imposed artificially to avoid damage, but rather is a natural consequence of the limited power resources available on the spacecraft. Therefore, the average-power constraint is a fundamental limit related to the conservation of energy and imposes a bound on the number of photons the transmitter can deliver per unit time. As before, modulation formats capable of maintaining high data throughput at the receiver under an average-power constraint, and at the required fidelity, are highly desirable.

1. The Case of Equal Bandwidths. If we require that all three schemes have equal bandwidths, i.e., equal slot durations, then, because compound-2 single-pulse and dual-pulse PPM schemes each have two slots filled per symbol, whereas the signals in conventional single-pulse PPM occupy only a single slot per symbol, in this case we have $K_s^{(A)} = K_s^{(B)} = K_s^{(C)}/2$, or, equivalently, $\lambda_s^{(A)} = \lambda_s^{(B)} = \lambda_s^{(C)}/2$. Thus, for an average-power constraint and equal transmission bandwidths, conventional single-pulse PPM requires twice the peak power of the other two schemes. Figure 5 is the analogous plot to Fig. 2 for the average-power-constraint case, where the abscissa now corresponds to the average energy per symbol, $E_s \left(= 2\lambda_s^{(A)}\tau = 2\lambda_s^{(B)}\tau = \lambda_s^{(C)}\tau\right)$, or, equivalently, the average power normalized (multiplied) by T_s. Since the Poisson distribution depends only on the average photon count parameter, K_s, we observe, as expected, that now conventional single-pulse PPM has a greater advantage than before, at the expense, however, of a doubled peak power.

Once again to take into account the difference in information throughputs of the three schemes, we proceed analogously to Fig. 3 and consider a plot of bit-error probability versus average energy per bit $E_b = E_s/N$. The relations between bit- and symbol-error probabilities are still given by Eqs. (36) through (38) but now, as was the case in Fig. 5, the effective K_s for the Poisson distribution of each of the two-pulse schemes is half that of the conventional single-pulse PPM scheme. The results are illustrated in Fig. 6. Here we see that dual-pulse PPM once again outperforms compound-2 single-pulse PPM but is still inferior to conventional single-pulse PPM. We reiterate the fact that the bit-error probability of compound-2 M-PPM is identical to that of conventional single-pulse $(M/2)$-PPM as explained in Footnote 4.

2. The Case of Equal Information Throughputs per Symbol. Once again we now compare the three schemes based on equal information throughputs as characterized by Eq. (5) [which in the previous section was shown to imply Eq. (39)] but still maintain the average-power constraint. In addition, in view of the peak-power inequality between single- and dual-pulse schemes, instead of Eq. (40) we now have

$$K_s^{(A)} = K_s^{(B)} = \frac{1}{2} K_s^{(C)} \tag{42}$$

Since the background radiation level is not affected by the nature (peak or average) of the power constraint imposed on the signal, the relation in Eq. (41) still applies here. Figure 7 is the analogous plot to Fig. 4 for the average-power-constraint case. Here we see that, despite the bandwidth advantage of the two-pulse

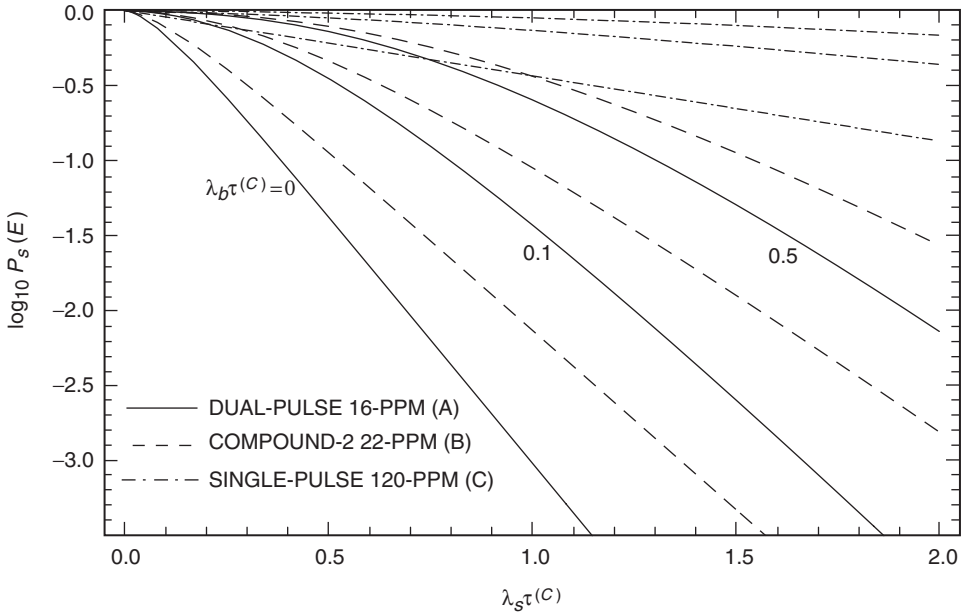

Fig. 4. Average symbol-error probability versus normalized peak power for conventional single, compound single, and dual-pulse PPM with normalized background power as a parameter; equal information throughputs.

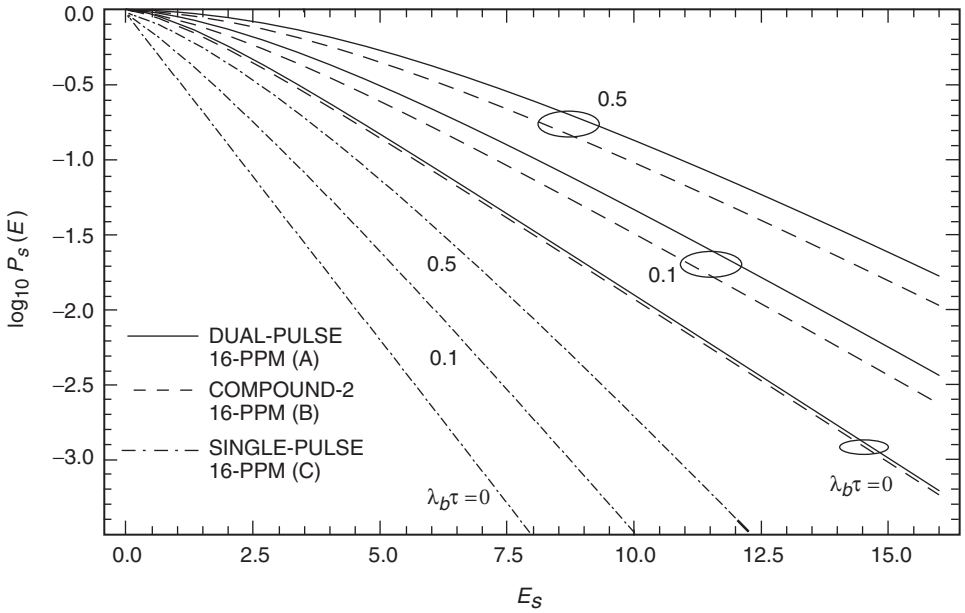

Fig. 5. Average symbol-error probability versus average energy per symbol for dual-pulse PPM with normalized background power as a parameter; equal bandwidths.

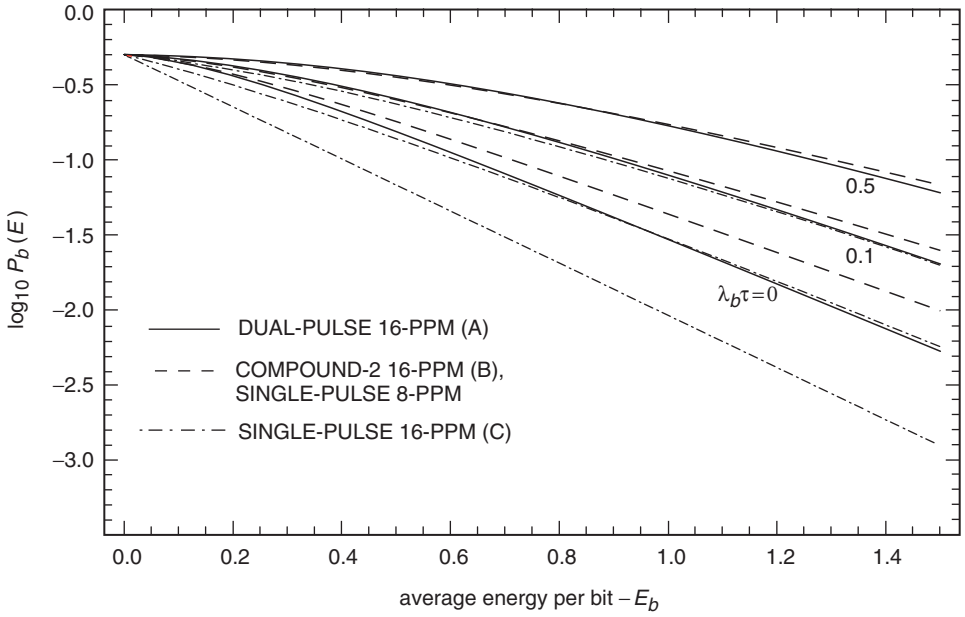

Fig. 6. Average bit-error probability versus normalized average power per bit for conventional single, compound single, and dual-pulse PPM with normalized background power as a parameter; equal bandwidths.

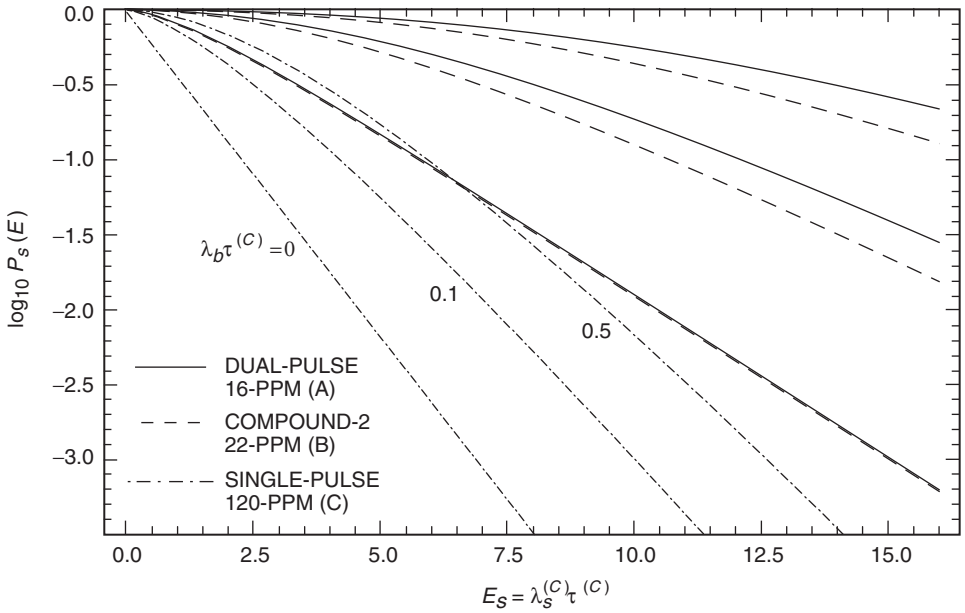

Fig. 7. Average symbol-error probability versus average energy per symbol for conventional single, compound single, and dual-pulse PPM with normalized background power as a parameter; equal information throughputs.

PPM schemes compared to that of conventional single-pulse PPM, the loss of 3 dB in the average signal photon count for the former compared to the latter, as predicted by Eq. (42), dominates the differences in their relative performance.

To take into account the differences in the bandwidth of the three schemes, we modify the comparison to allow for equal average symbol energy per slot time duration, K_s/τ, which is tantamount to assuming $\lambda_s^{(A)} = \lambda_s^{(B)} = (1/2)\lambda_s^{(C)}$. Equivalently, the relationship among the average photon counts results in a combination of Eqs. (40) and (42), namely,

$$\left.\begin{aligned} K_s^{(A)} &= \frac{1}{2} K_s^{(C)} \left(\frac{M^{(A)} - 1}{2} \right) \\ K_s^{(B)} &= \frac{1}{2} K_s^{(C)} \left(\frac{M^{(B)}}{4} \right) \end{aligned}\right\} \tag{43}$$

Once again the average photon count for the background noise in the three cases satisfies Eq. (41). Based on the above, we consider a plot of average symbol-error probability versus average symbol energy per slot time duration, where for convenience we fix the slot time of the conventional single-pulse PPM case, $\tau^{(C)}$. Such a comparison is illustrated in Fig. 8, where $P_s(E)$ is plotted versus $K_s^{(C)}/\tau^{(C)} = \lambda_s^{(C)}$ for a typical value of $\tau^{(C)} = 10^{-9}$. Here we see the superior performance of dual-pulse PPM over the other two schemes, brought about by the bandwidth saving.

As before, one could alternatively characterize the performance in terms of a plot of bit-error probability versus average energy (photons) per bit. Since, in the equal throughput case, the number of bits/symbol is the same for all three modulation schemes, e.g., $\log_2 M^{(C)}$, then the x-axis (abscissa) would merely scale by this factor. The conversion of the y-axis (ordinate) from symbol- to bit-error probability

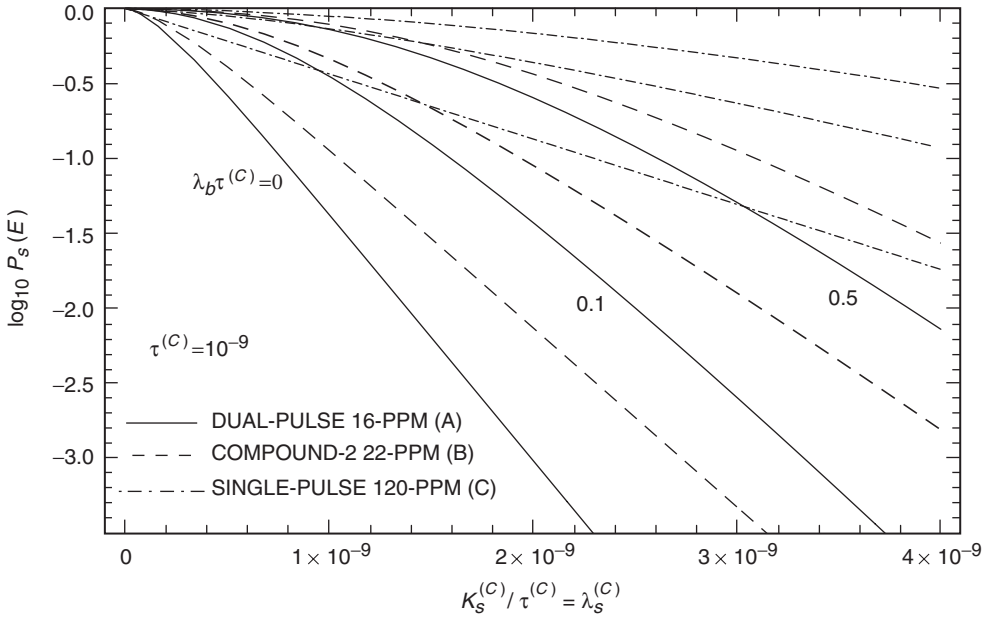

Fig. 8. Average symbol-error probability versus average symbol energy per slot time for conventional single, compound single, and dual-pulse PPM with normalized background power as a parameter; equal information throughputs.

would follow the relations in Eqs. (36) through (38). For $M^{(A)} = 16$, as is the case in Fig. 8, these conversions become $P_b(E) = (120/238)P_s(E)$ for conventional single-pulse PPM, $P_b(E) \cong (121/240)P_s(E)$ for compound-2 single-pulse PPM, and $P_b(E) \cong (120/238)P_s(E)$ for dual-pulse PPM all of which are very close to $P_b(E) = (1/2)P_s(E)$. Thus, in conclusion, a plot of bit-error probability versus average energy per slot time per bit would resemble Fig. 8 where the x-axis would be scaled (divided) by a factor of $\log_2 120$ and the y-axis by approximately a factor of 1/2.

VI. Conclusions

Higher-order PPM signaling has been examined and evaluated in terms of information throughput, bandwidth requirements, and error performance, under both peak- and average-power constraints. It was demonstrated that higher-order PPM, where multiple pulses are used per channel symbol, is a viable solution to bandwidth- and power-constrained optical communications, enabling higher data rates at a given bandwidth, without sacrificing bit-error-rate performance. Maximum-likelihood decision strategies were developed, and exact performance expressions for two-pulse PPM were derived. Two different forms of multi-pulse PPM signals were examined, one that is a direct extension of conventional single-pulse PPM, and which therefore could be substituted directly into existing single-pulse systems to enhance performance without the need for extensive redesign, and a more general form that employs a new detection strategy that is somewhat more complicated, but not prohibitively so. Both of these multi-pulse signaling formats, when operating with equal throughput/symbol and equal symbol rates, were shown to outperform conventional single-pulse PPM when operating under a peak-power constraint, by requiring up to 10 dB less transmitted signal peak power to attain comparable bit-error performance. This investigation has led to a promising new approach in signal design wherein communications system performance of more general modulation formats can be evaluated exactly in terms of fundamental system parameters, contributing to our understanding of the problem and thus enabling further modifications as needed, without relying entirely on complicated and costly computer simulations to evaluate each new point design.

References

[1] R. M. Gagliardi and S. Karp, *Optical Communications,* New York: Wiley, 1976.

[2] J. R. Pierce, "Optical Channels: Practical Limits with Photon Counting," *IEEE Trans. Commun.,* vol. COM-26, no. 12, pp. 1819–1821, December 1978.

[3] H. Sugiyama and K. Nosu, "MPPM: A Method of Improving the Band-Utilization Efficiency in Optical PPM," *Journal of Lightwave Tech.,* vol. 7, no. 3, pp. 465–472, March 1989.

[4] V. A. Vilnrotter and M. Srinivasan, "Adaptive Detector Arrays for Optical Communications Receivers," *IEEE Trans. Commun.,* vol. 50, no. 7, pp. 1091–1097, July 2002.

[5] J. I. Marcum, *Table of Q Functions,* U.S. Air Force Project RAND Research Memorandum M-339, ASTIA Document AD 1165451, Rand Corporation, Santa Monica, California, January 1, 1950.

[6] M. Abramowitz and I. A. Stegun, *Handbook of Mathematical Functions with Formulas, Graphs, and Mathematical Tables,* 9th ed., New York: Dover Press, 1972.

[7] C. Georghiades, "Modulation and Coding for Throughput-Efficient Optical Systems," *IEEE Trans. Inform. Theory,* vol. 40, no. 5, pp. 1313–1326, September 1994.

[8] M. K. Simon, S. M. Hinedi, and W. C. Lindsey, *Digital Communication Techniques: Signal Design and Detection,* Upper Saddle River, New Jersey: Prentice Hall, 1995.